Archives of Mechanics • Archiwum Mechaniki Stosowanej • 28, 2, pp. 171–188, Warszawa 1976

A crack-thermal stress problem in a doubly connected solid(*)

K. HERRMANN and R. KÜMMERLING (KARLSRUHE)

THIS paper presents the near-field solution for a Griffith-crack in a doubly connected thermoelastic solid which is subjected by a well-defined macroscopic thermal stress field. The crack-thermal stress problem is solved using the linear theory of quasi-static thermoelasticity as well as an analytical method which is based on the application of complex potentials and on the method of integral equations. The crack surface displacement, the elastic crack surface energy and also the opening-mode stress intensity factor were calculated. Several numerical results are given.

Praca niniejsza przedstawia rozwiązanie bliskiego zasięgu dla szczeliny Griffitha w dwuspójnym termosprężystym ciele stałym, w którym dobrze jest określone pole makroskopowych naprężeń cieplnych. Zagadnienie naprężenia termicznego szczeliny zostało rozwiązane w ramach liniowej quasi-statycznej teorii termosprężystości posługując się metodą analityczną, wykorzystującą potencjały zespolone i teorię równań całkowych. Obliczono przemieszczenie powierzchni szczeliny, energię sprężystą powierzchni szczeliny oraz współczynnik intensywności naprężenia otwarcia. Przedstawiono liczne wyniki numeryczne.

Настоящая работа представляет решение в близкой области для трещины Гриффита в двухсвязном термоупругом твердом теле, в котором хорошо определено поле макроскопических термических напряжений. Проблема термического напряжения трещины решена в рамках линейной квазистатической теории термоупругости, послуживаясь аналитическим методом использующем комплексные потенциалы и теорию интегральных уравнений. Вычислены перемещения поверхности трещины, упругая энергия поверхности трещины, а также коэффициент интенсивности напряжения открытия. Представлены многие численные результаты.

1. Introduction

THERMAL fracture of homogeneous and inhomogeneous solids was investigated theoretically and experimentally in the references [1–15]. It was shown by SIH [3] that in the case of thermal fracture crack-tip stress intensity factors can be defined corresponding to those for isothermal problems with applied forces. Further, for a crack-thermal stress problem, there exists also a characteristic $\varrho^{-1/2}$ — singularity at the crack tip, where ϱ means a local polar coordinate referred to the crack tip. EMERY [6] using a result of reference [16] for a two-dimensional edge crack in a half-space gave an approximative solution for two-dimensional cracks located at the inner and outer radii of thick hollow cylinders under transient heating conditions. The determination of the stress intensity factor was performed by using DUHAMEL'S theorem of linear superposition. Thereby the application of the mathematical method used for radial cracks in hollow cylinders depends in effect on the solution of the corresponding boundary-value problem for the thermal stresses in the uncracked solid. Several experimental results about fracture of brittle materials, especially silicate

(*) Dedicated to Prof. Dr. Witold NOWACKI on the occasion of his 65th birthday.

glasses, under the influence of thermal shocks can be found in reference [12], which deals also with the problem of thermal crack propagation. Thereby the crack velocity, the specific fracture energy as well as the stress intensity factor of a running crack in a suddenly cooled or heated plate were given in dependence of crack length. The crack velocity was evaluated by means of the so-called WALLNER-lines as well as using the ultrasonic method developed by KERKHOF [17, 18]. Finally, BREGMAN and KASSIR [14] dealt in a theoretical investigation with the problem of uniform heat flow disturbed by an insulated penny-shaped crack along the interface between two semi-infinite elastic media with different thermo-mechanical properties.

The objective of this paper is to present an additional contribution to the crack-thermal stress problem in a linear-elastic, homogeneous, isotropic, doubly connected solid. Therein the cohesive connection of the solid, a concentric hollow cylinder of infinite length with the elastic material constants E (YOUNG'S modulus), ν (POISSON'S ratio) and the thermal material constant α (linear coefficient of thermal expansion), is disturbed by an internal crack of short length $l = b\text{-}a$ with either $a, b < x_2$ or with $a, b > x_2$ in such a way that the crack tips $x_t = a$ and $x_t = b$ are far enough from the stress-free boundaries Γ_j $(j = 1, 2)$, (cf. Fig. 1). Further, at time $t = t^*$ the cracked solid, having for $t < t^*$ the temperature $T_e = 0$ of the surroundings, gets a thermal shock (cf. Fig. 1 for notation)

$$T(x, y) = \begin{cases} 0 & \text{for} \quad x < x_2, \\ T_0 & \text{for} \quad x > x_2, \end{cases} \tag{1.1}$$

at which we presume $x_2 = r_2 \cos\phi_2 > r_1$.

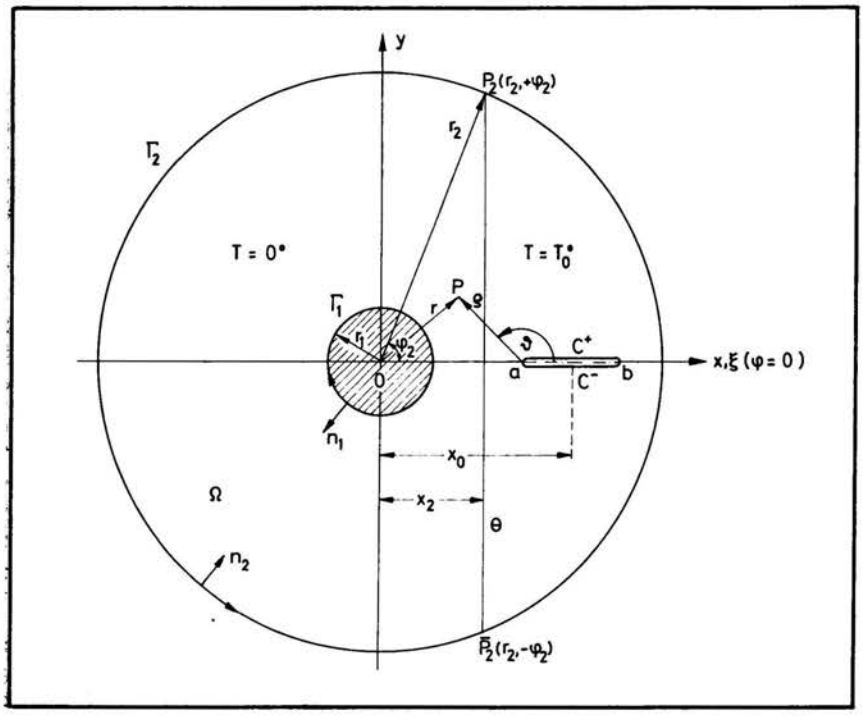

FIG. 1. Crack configuration in the cross-section of the doubly connected solid.

Owing to the complicated shape of the boundary of the cracked solid a closed solution of this crack-thermal stress problem cannot be obtained. Now from a physical point of view the stress and displacement state in the neighborhood of the crack tips as well as the crack surface energy required for the formation of new surfaces are of special interest. Hence in the following we seek for a near-field solution of the problem stated above, which allows the calculation of the crack surface displacement, the specific fracture energy as well as the stress intensity factor corresponding to Mode I displacement.

2. Basic equations

The self-stress state in the cracked solid induced by the thermal shock (1.1) has to fulfil the boundary conditions of the tension freedom on the entire boundary $\Gamma_1 \cup \Gamma_2 \cup C^+ \cup C^-$. Moreover, a requirement for the uniqueness of the displacement vector $\mathbf{u}$ must be added. Using the linear theory of quasi-static thermoelasticity for a plane strain state and assuming temperature independence of the elastic and thermal material constants as well as heat insulation of the solid with respect to its neighborhood, the thermal stress field existing in the cracked doubly connected solid can be decomposed into two parts:

1) a regular stress field in the uncracked doubly connected solid, and

2) a corrective stress field with two singularities at the crack tips of magnitude $\varrho^{-1/2}$, where ϱ is a local polar coordinate referred to the crack tip.

As it is noticed by KRÖNER [19], self-stresses induced in a solid by a heterogeneous temperature distribution can be integrated into the continuum theory of stationary dislocations. The basic equations read

$$\sigma_{ij} = 2\mu \left\{ \varepsilon_{ij} + \frac{\nu}{1-2\nu} \varepsilon_{kk} \delta_{ij} \right\}, \tag{2.1}$$

$$\sigma_{ij,i} = 0, \tag{2.2}$$

$$\varepsilon_{ijk}\varepsilon_{lmn}\varepsilon_{km,jn} = -\alpha \varepsilon_{ijk}\varepsilon_{lmn} T_{,jn}\delta_{km}, \tag{2.3}$$

where for the present the arbitrary heterogeneous temperature distribution function $T = T(x, y)$ belongs to class $C^{(2)}$ and ε_{ijk} means the asymmetrical LEVI-CIVITA tensor. Further, the sum of the incompatible strains ε_{ij} and of the incompatible extra-strains $\alpha T \delta_{ij}$ gives the compatible strains

$$e_{ij} = \varepsilon_{ij} + \alpha(T - T_e)\delta_{ij} \tag{2.4}$$

which are related to the undistorted initial state and derivable from a steady displacement vector $\mathbf{u}$. Moreover, the boundary conditions of the tension freedom of the surface ($n_i =$ = inner normal)

$$n_i \sigma_{ij} = 0 \tag{2.5}$$

are to be added.

3. Boundary-value problem of the uncracked solid

The regular self-stress field induced in the doubly connected uncracked solid by the thermal shock (1.1) given by means of DIRICHLET's discontinuous function as

$$T(r,\phi)=\frac{T_0}{2\pi i}\int\limits_{\uparrow}^{\uparrow}\frac{\exp z(r\cos\phi-r_2\cos\phi_2)}{z}\,dz,\qquad z=x+iy \tag{3.1}$$

can be obtained from the solution of the following boundary-value problem

$$\nabla^4\Phi_0(r,\phi)=0, \tag{3.2}$$

$$\nabla^2\Phi_1(r,\phi)=\frac{E\alpha}{1-\nu}T(r,\phi), \tag{3.3}$$

$$\left[\frac{1}{r^2}\frac{\partial^2\Phi(r,\phi)}{\partial\phi^2}+\frac{1}{r}\frac{\partial\Phi(r,\phi)}{\partial r}\right]_{r=r_j}=0,\qquad j=1,2 \tag{3.4}$$

$$\left[-\frac{\partial}{\partial r}\left\{\frac{1}{r}\frac{\partial\Phi(r,\phi)}{\partial\phi}\right\}\right]_{r=r_j}=0 \tag{3.5}$$

with the definition of the AIRY stress function

$$\Phi(r,\phi)=\Phi_0(r,\phi)-\Phi_1(r,\phi). \tag{3.6}$$

Further, the complete determination of the function $\Phi(r,\phi)$ requires the consideration of the displacement field. Because of the double connection of the uncracked solid it has to be proved that the displacement vector $\mathbf{u}$ is a unique function of the variables r and ϕ in the region Ω. The solution of the boundary-value problem (3.2)–(3.6), the AIRY stress function $\Phi(r,\phi)$, was given in reference [20] using complex potentials and proper power series. Considering the well-known formulae

$$\sigma^r_{rr}(r,\phi)=\frac{1}{r^2}\frac{\partial^2\Phi(r,\phi)}{\partial\phi^2}+\frac{1}{r}\frac{\partial\Phi(r,\phi)}{\partial r}, \tag{3.7}$$

$$\sigma^r_{\varphi\varphi}(r,\phi)=\frac{\partial^2\Phi(r,\phi)}{\partial r^2}, \tag{3.8}$$

$$\sigma^r_{r\varphi}(r,\phi)=-\frac{\partial}{\partial r}\left\{\frac{1}{r}\frac{\partial\Phi(r,\phi)}{\partial\phi}\right\}, \tag{3.9}$$

the regular stress state belonging to the AIRY stress function $\Phi(r,\phi)$ can be calculated. The corresponding expressions were presented in the paper cited above. Then the stress σ^r_{yy} on the prospective crack line has the shape

$$\begin{aligned}\sigma^r_{yy}(\tilde{x},0)=\overset{1}{\sigma}{}^r_{yy}(\tilde{x},0)+\overset{2}{\sigma}{}^r_{yy}(\tilde{x},0)=\overline{M}\Big\{&\overset{0}{P}+\overset{1}{P}\tilde{x}^{-4}+\overset{0}{A}\tilde{r}_1^2\tilde{x}^{-2}+\overset{2}{P}\tilde{x}^2\\&+\sum_{n=2}^{\infty}\frac{1}{2\overline{\Delta}^{(2n)}}(P^3_{2n}\tilde{x}^{-2n-2}-P^4_{2n}\tilde{x}^{-2n}+P^5_{2n}\tilde{x}^{2n-2}-P^6_{2n}\tilde{x}^{2n})\Big\}+\overline{M}\Big\{\overset{2}{Q}\tilde{x}^{-3}\\&+\overset{1}{Q}\tilde{x}+\sum_{n=1}^{\infty}\frac{1}{2\overline{\Delta}^{(2n+1)}}(P^3_{2n+1}\tilde{x}^{-2n-3}-P^4_{2n+1}\tilde{x}^{-2n-1}+P^5_{2n+1}\tilde{x}^{2n-1}-P^6_{2n+1}\tilde{x}^{2n+1})\Big\},\end{aligned} \tag{3.10}$$

where the two stresses $\overset{1}{\sigma}{}^r_{yy}$ and $\overset{2}{\sigma}{}^r_{yy}$ correspond to the even and to the odd parts of the stress $\sigma^r_{yy}(\tilde{x}, 0)$. The meaning of the abbreviations used in the Eq. (3.10) is given in the appendix I, formulae (A.I.1)–(A.I.7). The sign of the stress $\sigma^r_{yy}(\tilde{x}, 0)$ decides, whether a crack located at $a \leqslant x \leqslant b$, $y = 0$ will be open or tend to close. Opening takes place only if $\sigma^r_{yy}(\tilde{x}, 0)$ is a tension over the prospective crack line. Figure 2 shows the distribution of the stress

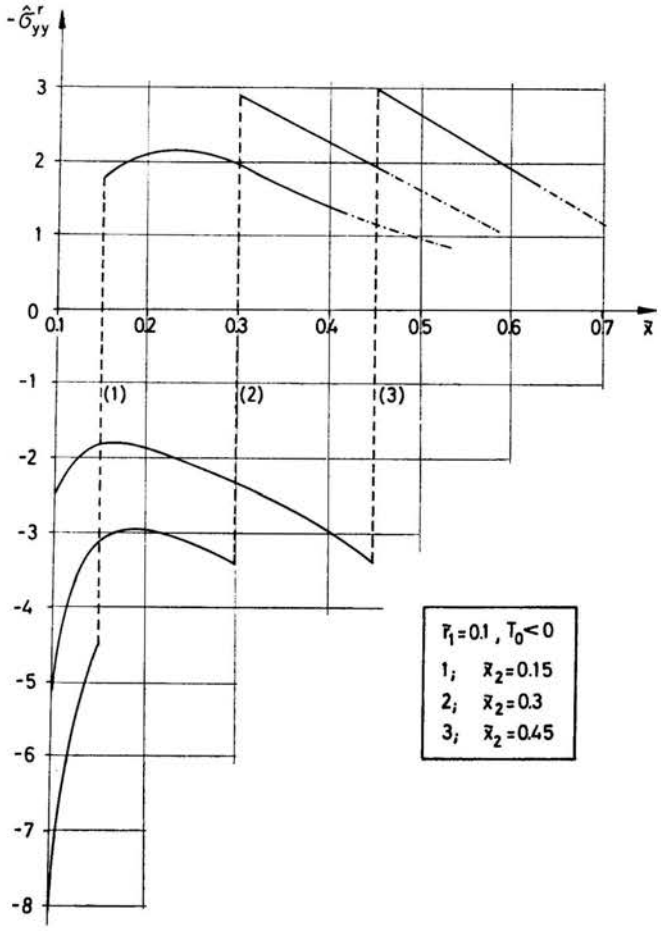

FIG. 2. Normal stress distribution in the symmetry line $y = 0$ of the uncracked solid in the environment of the discontinuity area of the temperature distribution.

$\sigma^r_{yy}(\tilde{x}, 0)$ in the symmetry line $y = 0$ in the environment of the discontinuity area θ of the temperature distribution for $T_0 < 0$ without consideration of the material factor $|\overline{M}|$.

It can be seen that the stress experiences a change of sign at $\tilde{x} = \tilde{x}_2$. Therefore a crack going through the discontinuity area θ of the temperature distribution would be partially closed.

4. Mixed boundary-value problem for the corrective stress field

The corrective stress field arises due to a stress distribution

$$\sigma^c_{yy}(x, 0) = -\sigma^r_{yy}(x, 0), \qquad a \leqslant x \leqslant b; \tag{4.1}$$

$$\sigma^c_{xy}(x, 0) = 0, \tag{4.2}$$

along the faces $C^+ \cup C^-$ of the crack. Moreover, the corrective stress field has to satisfy the conditions of the tension freedom on the boundary $\Gamma_1 \cup \Gamma_2$

$$\sigma^c_{rr}(r_j, \phi) = 0, \qquad j = 1, 2. \tag{4.3}$$

$$\sigma^c_{r\varphi}(r_j, \phi) = 0, \tag{4.4}$$

A closed solution of the boundary-value problem stated in the Eqs. (4.1)–(4.4) cannot be given because of the complicated shape of the boundary of the cracked solid. But by assuming a small crack with $l \ll (r_2 - r_1)$ and with crack tips far enough from the surfaces Γ_1 and Γ_2 according to the inequalities $l \ll (a - r_1)$ and $l \ll (r_2 - b)$, an approximative expression of the corrective stress field can be obtained from the solution of the following mixed boundary-value problem

$$\sigma^c_{yy}(\xi, 0) = -\sigma^r_{yy}(\xi, 0), \quad y = 0, |\xi| \leqslant \delta, \tag{4.5}$$

$$\sigma^c_{xy}(\xi, 0) = 0, \quad y = 0, \forall \xi, \tag{4.6}$$

$$u^c_y(\xi, 0) = 0, \quad y = 0, |\xi| > \delta, \tag{4.7}$$

with the abbreviations to apply

$$\xi = \tilde{x} - \tilde{x}_0, \quad \tilde{x}_0 = \frac{a+b}{2r_2}, \quad \delta = \frac{b-a}{2r_2}. \tag{4.8}$$

Besides, the crack is embedded in an infinite medium, at which the crack faces $C^+ \cup C^-$ experience the stress field due to the thermally stressed geometry in Fig. 1. Considering the assumptions made about the position and the length of the internal crack this procedure should be justified because, from a physical point of view, the corrective stress field represents a small perturbation, at which only the stress and displacement state in the neighbourhood of the crack gives a remarkable contribution. Now a solution of the mixed boundary-value problem (4.5)–(4.7) can be given using an analytical method [21] based on the application of complex variable technique and on the method of integral equations. Therein the expressions for the stress σ^c_{yy} and for the displacement u^c_y on the line $z = \bar{z}$ can be represented by means of one complex potential $\Psi(z)$ according to

$$\sigma^c_{yy}(\xi, 0) = 2\{\Psi'(z) + \overline{\Psi}'(\bar{z})\}, \tag{4.9}$$

$$u^c_y(\xi, 0) = \frac{2(1-\nu)}{\mu} i \{\overline{\Psi}(\bar{z}) - \Psi(z)\}, \tag{4.10}$$

provided the following conditions hold for $y \to \pm 0$:

$$y\overline{\Psi}'(\bar{z}) \to 0, \quad y\overline{\Psi}''(\bar{z}) \to 0. \tag{4.11}$$

Moreover, they have to hold for $|z| \to \infty$: $\Psi'(z) = 0(1/z^2)$. Then the complex potential $\Psi(z)$ can be given by means of the integral

$$\Psi(z) = \int_0^{\delta} \frac{\Lambda_1(t)+z\Lambda_2(t)}{\sqrt{z^2-t^2}}\, dt, \tag{4.12}$$

where the functions $\Lambda_j(t)$, $(j = 1, 2)$ are the solutions of a pair of ABEL type integral equations

$$4\frac{d}{d\xi}\int_0^{\xi} \frac{\Lambda_1(t)}{\sqrt{\xi^2-t^2}}\, dt = -\omega_1(\xi), \tag{4.13}$$

$$0 \leqslant \xi \leqslant \delta.$$

$$4\frac{d}{d\xi}\int_0^{\xi} \frac{\xi\Lambda_2(t)}{\sqrt{\xi^2-t^2}}\, dt = -\omega_2(\xi), \tag{4.14}$$

Therein the right-hand sides of the integral equations (4.13)–(4.14) leaving out signs correspond to the even part $\overset{1}{\sigma}{}^r_{yy}(\tilde{x}, 0)$ and to the odd part $\overset{2}{\sigma}{}^r_{yy}(\tilde{x}, 0)$ of the stress $\sigma^r_{yy}(\tilde{x}, 0)$ according to the Eq. (3.10). Using the latter equation and by truncation of the power series after the second term, the solutions of the integral equations (4.13)–(4.14) have the following shape

$$\begin{aligned}\Lambda_1(t) = -\frac{t}{2\pi}\int_0^t \frac{\omega_1(u)}{\sqrt{t^2-u^2}}\, du = -\frac{\bar{M}t}{2\pi}\Big\{&\frac{\pi}{2}\overset{0}{P}+\overset{0}{A}r_1^2 J_1 \\ &+\left(\overset{1}{P}-\frac{1}{2\bar{\Delta}^{(4)}}P_4^4\right)J_2+\frac{1}{2}\left(\frac{1}{\bar{\Delta}^{(4)}}P_4^3-\frac{1}{\bar{\Delta}^{(6)}}P_6^4\right)J_3+\frac{1}{2\bar{\Delta}^{(6)}}P_6^3 J_4 \\ &+\left(\overset{2}{P}+\frac{1}{2\bar{\Delta}^{(4)}}P_4^5\right)J_{-1}+\frac{1}{2}\left(\frac{1}{\bar{\Delta}^{(6)}}P_6^5-\frac{1}{\bar{\Delta}^{(4)}}P_4^6\right)J_{-2}-\frac{1}{2\bar{\Delta}^{(6)}}P_6^6 J_{-3}\Big\},\end{aligned} \tag{4.15}$$

$$\begin{aligned}\Lambda_2(t) = -\frac{1}{2\pi t}\int_0^t \frac{u\omega_2(u)}{\sqrt{t^2-u^2}}\, du = -\frac{\bar{M}}{2\pi t}\Big\{&\left(\overset{1}{Q}+\frac{1}{2\bar{\Delta}^{(3)}}P_3^5\right)L_0 \\ &+\left(\overset{2}{Q}-\frac{1}{2\bar{\Delta}^{(3)}}P_3^4\right)L_2+\frac{1}{2}\left(\frac{1}{\bar{\Delta}^{(3)}}P_3^3-\frac{1}{\bar{\Delta}^{(5)}}P_5^4\right)L_3+\frac{1}{2\bar{\Delta}^{(5)}}P_5^3 L_4 \\ &+\frac{1}{2}\left(\frac{1}{\bar{\Delta}^{(5)}}P_5^5-\frac{1}{\bar{\Delta}^{(3)}}P_3^6\right)L_{-1}-\frac{1}{2\bar{\Delta}^{(5)}}P_5^6 L_{-2}\Big\},\end{aligned} \tag{4.16}$$

where the applied abbreviations can be found in the appendix I, formulae (A.I.1)–(A.I.7) and in the appendix II, formulae (A.II.1). Finally, by means of the solutions (4.15) and (4.16) of the integral equations (4.13) and (4.14) and using the formulae (4.10) and (4.12), one obtains the following real integral for the desired crack surface displacement of the upper face C^+ of the crack

$$\begin{aligned}u_y^c(\xi, 0) = -\frac{4(1-\nu)}{\mu}\int_{|\xi|}^{\delta} \frac{\Lambda_1(t)+\xi\Lambda_2(t)}{\sqrt{t^2-\xi^2}}\, dt = \frac{2}{\pi^2}(1+\nu)\alpha T_0\Big\{&J_3^0(S_8+\xi T_8) \\ &+\sum_{m=1}^{7}\left[\left(\frac{\pi}{2}J_1^m-J_2^m\right)(S_m+\xi T_m)+J_3^m(S_{m+8}+\xi T_{m+8})+J_4^m(S_{m+15}+\xi T_{m+15})\right]\Big\}.\end{aligned} \tag{4.17}$$

The abbreviations used in formulae (4.17) are defined in the appendix II, formulae (A.II.1)–(A.II.4).

By means of the crack surface displacement (4.17), the elastic surface energy required for the formation of new surfaces $C^+ \cup C^-$ in a specimen of unit thickness can be given according to the formula

$$U = -\int_{-\delta}^{\delta} \sigma_{yy}^c(\xi, 0) u_y^c(\xi, 0) d\xi. \tag{4.18}$$

Further, the strain energy release rate for the Mode I displacement can be obtained, which is defined by the integral

$$G_I = -\frac{1}{2}\frac{\partial}{\partial \delta}\int_{-\delta}^{\delta} \sigma_{yy}^c(\xi, 0) u_y^c(\xi, 0) d\xi. \tag{4.19}$$

The integrals in the formulae (4.18) and (4.19) cannot be expressed by a finite combination of elementary functions. Therefore the calculation has to be performed numerically. Finally, by using formula (4.19) and the IRWIN-relation

$$G_I = \frac{1-\nu^2}{E} K_I^2, \tag{4.20}$$

the opening-mode stress intensity factor can be given.

According to the formulae (4.19) and (4.20) the expressions for the strain energy release rate G_I and for the stress intensity factor K_I become functions of the quantities δ (half of the crack length), $\tilde{x}_0$ (position of the centre of the crack), $\tilde{x}_2$ (position of the discontinuity area of temperature) as well as of the temperature T_0. Thereby both formulae mentioned above are related to the crack tip which is most vulnerable to propagate. The latter behaviour is dependent on the position of the corresponding crack tip relative to the discontinuity area θ of the temperature and on the stress distribution σ_{yy}^r acting on the prospective crack line (cf. Fig. 2). Therefore the Figs. 7–9 given in chapter 5 show the energy release rate and the opening-mode stress intensity factor related to the crack tip which is most vulnerable to propagate in dependence on crack length and for several materials. In case of Fig. 8 for instance the crack tip mentioned above lies at point $x_t = a$ because the position of the crack, ($\tilde{x}_0 = 0.40$), is on the right-hand side of the discontinuity area θ, ($\tilde{x}_2 = 0.30$), and by consideration of the stress distribution σ_{yy}^r (cf. Fig. 2) acting on the prospective crack line for this crack tip only the stress intensity factor K_I increases with increasing crack length. Similar considerations lead to the results shown in Figs. 7 and 9. As a further example Fig. 10 shows the calculated values of the stress intensity factor K_I of the material PMMA 233 attached to the crack tips $x_t = a$ and $x_t = b$, respectively, for several positions of the crack with respect to the discontinuity area θ of the temperature. Finally, the respective second value of the stress intensity factor can be obtained by letting the crack length unaltered and by an appropriate variation of the parameter $\tilde{x}_0$. Of course, due to the stress distribution σ_{yy}^r (cf. Fig. 2) acting on the prospective crack line, the stress intensity factors at both crack tips are different in general, but in spite of the asymmetric behaviour of the crack surface displacement, as is shown in Figs. 3–5,

the differences between the values of the stress intensity factor K_I at point $x_t = a$ and $x_t = b$, respectively, become small because of the assumptions about the position and the length of the crack made in chapter 4.

5. Numerical results and discussions

The numerical calculations were performed on the computer UNIVAC 1108 of the University of Karlsruhe.

According to formula (4.17) Figs. 3–5 show the displacement distribution u_y^c of the upper crack face C^+ for several crack lengths and with the quantities $\tilde{x}_2$ and $\tilde{x}_0$ as parameters without consideration of the material factor $|\overline{N}| = \frac{2}{\pi^2}(1+\nu)\alpha|T_0|$. The curves have a remarkable asymmetry which can be explained according to Fig. 2 by the action of the stress distribution σ_{yy}^r along the crack line. Further it should be noticed that, due to the truncation of the power series of the stresses $\overset{1}{\sigma}{}_{yy}^r$ and $\overset{2}{\sigma}{}_{yy}^r$, the even and the odd parts of the regular stress distribution $\sigma_{yy}^r(\tilde{x}, 0)$, (cf. formula (3.10)), the numerical calculation of the crack surface displacement gives a discontinuity at point $\xi = 0$, that means, u_y^c goes to infinity there. From a physical point of view this mathematical discontinuity is unrealistic and therefore as value at point $\xi = 0$ the limit value was chosen, which is obtainable by approximation from $\xi < 0$ and $\xi > 0$, respectively. Further, the numerical calculation error of the stress $\hat{\sigma}_{yy}^r$ which influences also the value of the crack surface displacement becomes smaller if the discontinuity area θ of the temperature distribution approaches the outer surface Γ_2. For example, the error of calculation is smaller than 6% for $\tilde{x}_2 = 0.15$ and $\tilde{x} \leqslant 0.475$, smaller than 2,5% for $\tilde{x}_2 = 0.3$ and $\tilde{x} \leqslant 0.475$ and smaller than 0.2% for $\tilde{x}_2 = 0.45$ and $\tilde{x} \leqslant 0.375$. By contrast, the error of calculation becomes greater if for a fixed value of $\tilde{x}_2$ the value of $\tilde{x}$ goes to one. Therein all calculations were performed for a radius ratio $\tilde{r}_1 = 0.1$.

By means of the crack surface displacement u_y^c the elastic surface energy required for the formation of new surfaces $C^+ \cup C^-$ can be calculated according to formula (4.18). Figure 6 gives the value of the crack surface energy $\hat{U} = U/\overline{MN}$ for several crack lengths ($\delta_{max} = 2.5 \cdot 10^{-2}$) and with the quantities $\tilde{x}_0$ and $\tilde{x}_2$ as parameters. It can be seen that the value of $\hat{U}$ increases with increasing crack length.

Further, Fig. 7 shows the strain energy release rate $\hat{G}_I$ in dependence on crack length and with the same parameters as for the calculation of $\hat{U}$.

Finally, the knowledge of the specific fracture energy also allows the calculation of the stress intensity factor according to IRVIN's formula (4.20). Figures 8–9 give the opening-mode stress intensity factor K_I for several materials by consideration of the temperature dependence on the elastic and thermal material constants in dependence on crack length and with the quantities $\tilde{x}_0$ and $\tilde{x}_2$ as well as the temperature T_0 as parameters. Thereby Fig. 8 shows that the stress intensity factor increases with increasing crack length and with a decreasing value of the temperature T_0.

Because of the position of the crack on the right-hand side of the discontinuity area θ, a crack opening due to tensile stresses takes place only if the temperature T_0 is negative (cf. Fig. 2). It should be noticed that the convergence of the numerical calculations be-

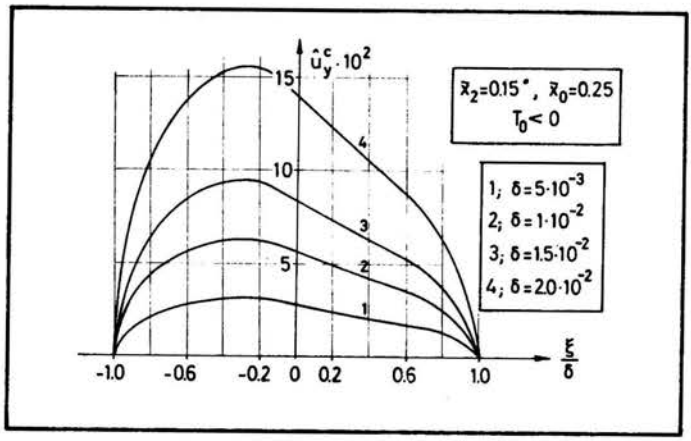

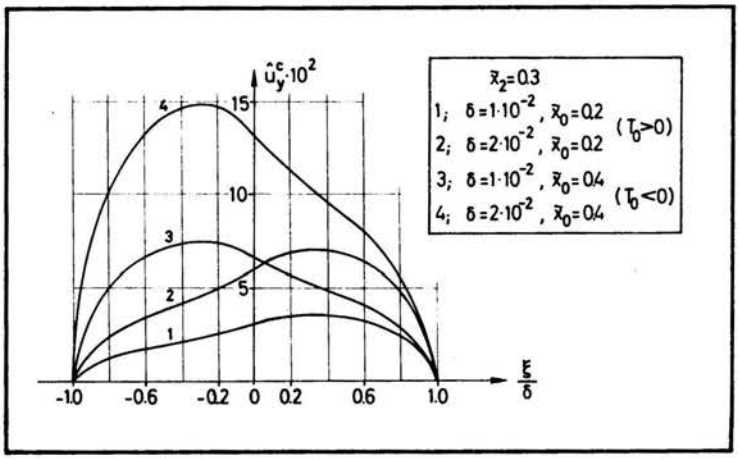

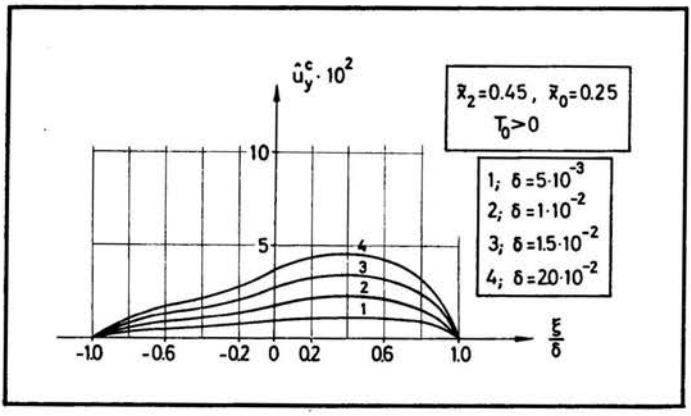

FIGS. 3–5. Crack surface displacement of the upper crack face C^+ for several crack lengths and different positions of the centre of the crack as well as of the discontinuity area of thet emperature distribution.

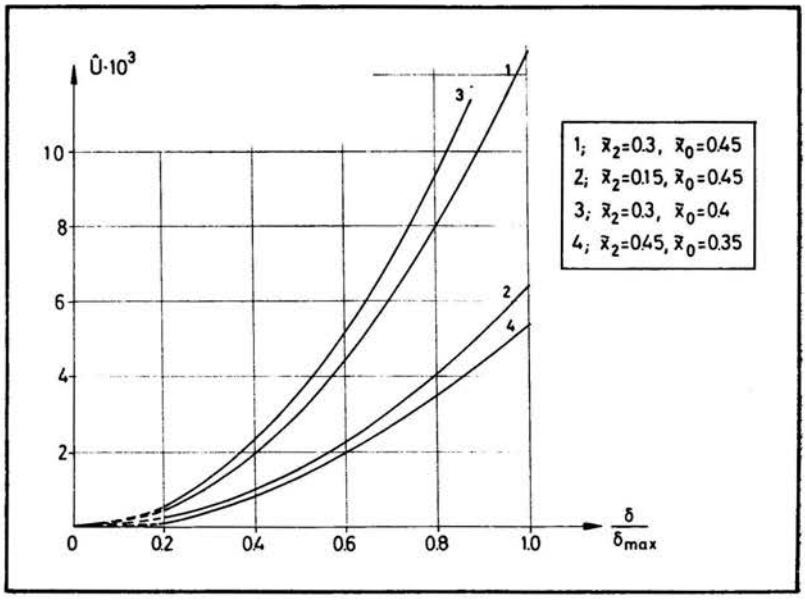

FIG. 6. Elastic crack surface energy in dependence on crack length.

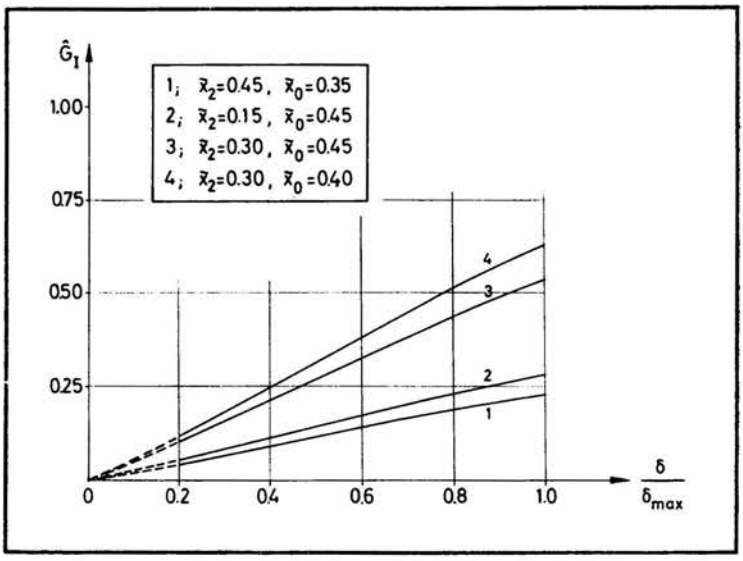

FIG. 7. Specific fracture energy at the crack tips $x_t = a$ (graphs 2, 3, 4) and $x_t = b$ (graph 1), respectively, in dependence on crack length.

comes weaker if the crack length becomes very small. Therefore for $\delta/\delta_{max} < 0.2$ the values of the stress intensity factor K_I were obtained by an extrapolation. Figure 9 shows the opening-mode stress intensity factor for three different materials, the optical glasses LASF 1 and FK 50 as well as PMMA 233.

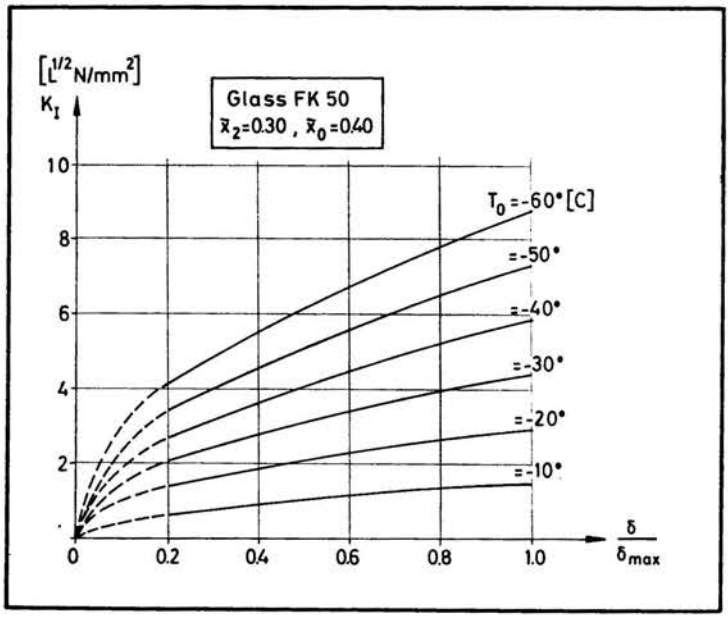

FIG. 8. Opening-mode stress intensity factor at the crack tip $x_t = a$ of the optical glass FK 50 in dependence on crack length for a special position of the centre of the crack and with the temperature T_0 as a parameter.

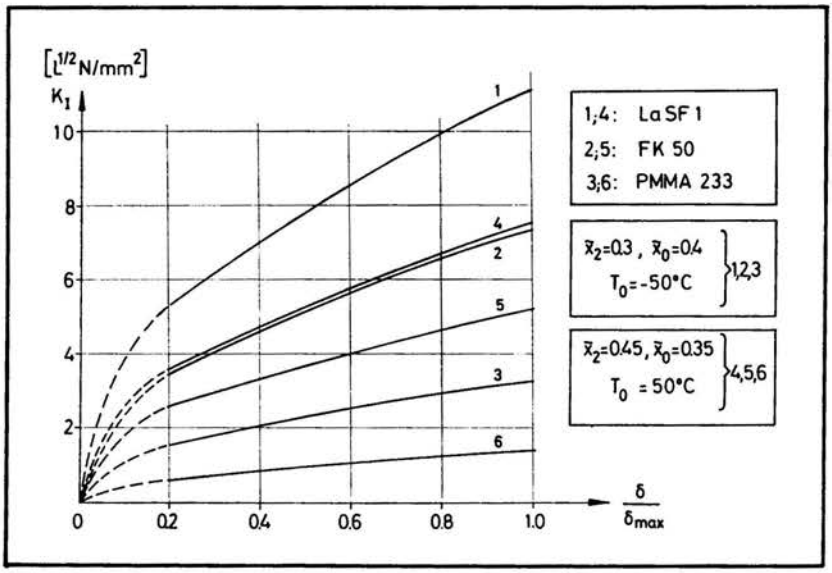

FIG. 9. Stress intensity factor at the crack tips $x_t = a$ (graphs 1, 2, 3) and $x_t = b$ (graphs 4,5, 6), respectively, of three different materials in dependence on crack lenglh.

It can be seen from Fig. 9 that the K_I-value of Polymethylmethacryalate for both positions of a crack is smaller than in the other two cases in spite of its high coefficient of thermal expansion because PMMA is relatively soft. Finally, Fig. 10 shows the value of the

PMMA 233
$\bar{r}_1 = 0.1$, $\bar{r}_2 = 0.3$
$T_0 = \pm 50°C$

$\bar{x}_0$	δ	K_I	x_t
0.15	0.020 0.025	1.45 1.82	a
0.20	0.020 0.025	1.31 1.68	b
0.40	0.020 0.025	2.93 3.24	a
0.45	0.020 0.025	2.69 2.98	a

FIG. 10. Stress intensity factor at the crack tips $x_t = a$ and $x_t = b$, respectively, of PMMA 233 in dependence on the position of the centre of the crack and with the crack length as a parameter.

stress intensity factor of PMMA 233 in dependence on the position of the centre of the crack and with δ (half of the crack length) as a parameter. By means of Fig. 2 this table gives the possibility to attach the calculated values of K_I to the crack tips $x_t = a$ and $x_t = b$, respectively. It should be remarked that the stress intensity factors at both crack tips are different in general, but this difference is not too large due to the chosen position and the length of the crack.

In case of cracks of great length where the surfaces Γ_1 and Γ_2, respectively, strongly influence the stress concentration at both crack tips $x_t = a$ and $x_t = b$, the analytical method of reference [21] cannot be used any longer. Then a determination of the crack surface displacement caused by the tensile stress $\sigma^r_{yy}(x, 0)$ acting on the crack line $a \leqslant x \leqslant b$, $y = 0$ can for example take place by the finite element method. In this case, using a deformation conforming finite element program, only the displacements of nodal points on the crack face are of interest. Further, the displacements will be small with increased distance from the crack, since only the two crack faces are subjected to loading.

Finally, the calculation of the opening-mode stress intensity factor could be performed also by means of the well-known J-integral [22]. Using a proposal made in reference [23] a rectangular integration-path far enough from the crack tip can be chosen. Then the singular stress field at the crack tip does not influence essentially the behaviour of the material along this way.

From a physical point of view the crack-thermal stress problem treated in the previous sections is of significance for the study of the behaviour of small initial cracks in a brittle

material stressed by well-defined macroscopic thermal stresses. Hence for a judgment of the strength of such a material containing subcritical cracks, the knowledge of the elastic crack surface energy required for the formation of new surfaces is important. This energy represents a part of the elastic self-stress energy stored up in the originally uncracked specimen. Hence in case of a crack formation in a primarily uncracked solid a relaxation of the specimen takes place up to the point where the crack is arrested due to the shortness of the elastic self-stress energy. Thus self-stress fracture represents the inverse case of fracture under the influence of external loading concerning the velocity of crack propagation.

Appendix I

The applied abbreviations in the Eq. (3.10) are:

(A.I.1.a-d) $$\overline{M} = \frac{E\alpha T_0}{2\pi(1-\nu)}, \quad C = \begin{cases} 0 \text{ for } x < x_2 \\ 1 \text{ for } x > x_2 \end{cases}, \quad \tilde{x} = \frac{x}{r_2}, \quad \tilde{r}_1 = \frac{r_1}{r_2};$$

$$\overset{0}{P} = -\pi C + \overset{0}{A} + \frac{1}{\overline{\Delta}^{(2)}}(\overset{0}{B} + \overset{0}{C} + \overset{0}{F} + \overset{0}{J}), \quad \overset{1}{P} = \frac{1}{\overline{\Delta}^{(2)}}(\overset{0}{D} + \overset{0}{G} - \overset{0}{K}),$$

(A.I.2.a-g) $$\overset{2}{P} = \frac{1}{\overline{\Delta}^{(2)}}(-\overset{0}{E} + \overset{0}{H} - \overset{0}{L}), \quad P_m^3 = A_{m+2}N_m^1 + 2B_m N_m^5 + D_{m+2}N_m^{10},$$

$$P_m^4 = A_{m+2}N_m^2 + 2B_m N_m^6 + D_{m+2}N_m^{11}, \quad P_m^5 = A_{m+2}N_m^3 + 2B_m N_m^7 + D_{m+2}N_m^{12},$$

$$P_m^6 = A_{m+2}N_m^4 + 2B_m N_m^8 - 2C_{m+2}N_m^9 + D_{m+2}N_m^{13}, \quad m \geqslant 3;$$

(A.I.3.a-b) $$\overset{1}{Q} = 3\overset{0}{M}, \quad \overset{2}{Q} = \tilde{r}_1^4 \overset{0}{M};$$

(A.I.4.a-l) $$\overset{0}{A} = \frac{1}{2(1-\tilde{r}_1^2)}(2\phi_2 - \sin 2\phi_2), \quad \overset{0}{B} = -\pi C(\tilde{r}_1^{-6} - 4\tilde{r}_1^{-4} + 6\tilde{r}_1^{-2} + \tilde{r}_1^2 - 4);$$

$$\overset{0}{C} = \phi_2(\tilde{r}_1^{-6} + 3\tilde{r}_1^{-2} - 4), \quad \overset{0}{D} = 3\phi_2(\tilde{r}_1^{-2} - \tilde{r}_1^2), \quad \overset{0}{E} = 12\phi_2(\tilde{r}_1^{-4} - \tilde{r}_1^{-2}),$$

$$\overset{0}{F} = \sin 2\phi_2(-\tilde{r}_1^{-6} - \tilde{r}_1^{-2} + 2), \quad \overset{0}{G} = \sin 2\phi_2(2 - 3\tilde{r}_1^{-2} + \tilde{r}_1^2),$$

$$\overset{0}{H} = 2\sin 2\phi_2(\tilde{r}_1^{-6} + 2\tilde{r}_1^{-4} - 3\tilde{r}_1^{-2}), \quad \overset{0}{J} = \frac{1}{4}\sin 4\phi_2(\tilde{r}_1^{-6} - \tilde{r}_1^{-2}),$$

$$\overset{0}{K} = \frac{1}{4}\sin 4\phi_2(4 - 3\tilde{r}_1^{-2} - \tilde{r}_1^2), \quad \overset{0}{L} = \sin 4\phi_2(\tilde{r}_1^{-6} - \tilde{r}_1^{-4}),$$

$$\overset{0}{M} = \frac{1}{3(1-\tilde{r}_1^4)}(3\sin\phi_2 - \sin 3\phi_2);$$

(A.I.5.a-b)
$$\bar{\Delta}^{(2)} = \tilde{r}_1^{-6} - 4\tilde{r}_1^{-4} + 6\tilde{r}_1^{-2} + \tilde{r}_1^{2} - 4,$$
$$\bar{\Delta}^{(m)} = \tilde{r}_1^{-2m} - m^2\tilde{r}_1^{-2} - m^2\tilde{r}_1^{2} + \tilde{r}_1^{2m} + 2(m^2-1), \quad m > 2;$$

(A.I.6.a-d)
$$A_m = \frac{m-4}{m-2}\sin(m-2)\phi_2 - \frac{m-4}{m}\sin m\phi_2,$$
$$B_m = \frac{1}{m-2}\sin(m-2)\phi_2 - \sin m\phi_2 + \frac{m-1}{m+2}\sin(m+2)\phi_2,$$
$$C_m = \frac{m}{m-2}\sin(m-2)\phi_2 - \sin m\phi_2,$$
$$D_m = \sin(m-2)\phi_2 - \frac{m-2}{m}\sin m\phi_2, \quad m \geqslant 3;$$

(A.I.7.a-m)
$$N_m^1 = m(\tilde{r}_1^2 + m\tilde{r}_1^{2m} - (m+1)\tilde{r}_1^{2m+2}), \quad N_m^2 = (m-2)(1+(m-1)\tilde{r}_1^{2m} - m\tilde{r}_1^{2m+2}),$$
$$N_m^3 = m(m+(1-m)\tilde{r}_1^2 - \tilde{r}_1^{2m+2}), \quad N_m^4 = (m+2)(m+1-m\tilde{r}_1^2 - \tilde{r}_1^{2m}),$$
$$N_m^5 = (m+1)(1-\tilde{r}_1^{2m}), \quad N_m^6 = (m-2)(\tilde{r}_1^{-2} - \tilde{r}_1^{2m}),$$
$$N_m^7 = m^2 - 1 + \tilde{r}_1^{-2m} - m^2\tilde{r}_1^2, \quad N_m^8 = (m^2+3m+2)(\tilde{r}_1^{-2} - 1),$$
$$N_m^9 = 2(m^2-1) + \tilde{r}_1^{-2m} - m^2\tilde{r}_1^{-2} - m^2\tilde{r}_1^2 + \tilde{r}_1^{2m},$$
$$N_m^{10} = (m+2)\tilde{r}_1^2 - m^2\tilde{r}_1^{2m} + (m^2-m-2)\tilde{r}_1^{2m+2},$$
$$N_m^{11} = (m-2)(1+(1-m)\tilde{r}_1^{2m} + (m-2)\tilde{r}_1^{2m+2}),$$
$$N_m^{12} = m^2 - (m^2+m-2)\tilde{r}_1^2 + (m-2)\tilde{r}_1^{2m+2},$$
$$N_m^{13} = (m+2)(m+1-(m+2)\tilde{r}_1^2 + \tilde{r}_1^{2m}), \quad m \geqslant 3.$$

Appendix II

The abbreviations used in the formulae (4.15)–(4.17) mean:

(A.II.1.a-b)
$$\int_0^t \frac{du}{(\tilde{x}_0+u)^{2m}\sqrt{t^2-u^2}} = J_m, \quad m = -3, -2, -1, 1, 2, 3, 4,$$
$$\int_0^t \frac{udu}{(\tilde{x}_0+u)^{2m-1}\sqrt{t^2-u^2}} = L_m, \quad m = -2, -1, 0, 2, 3, 4;$$

(A.II.2.a-b)
$$\int_{|\xi|}^{\delta} \frac{tdt}{(\tilde{x}_0^2-t^2)^m\sqrt{(\tilde{x}_0^2-t^2)(t^2-\xi^2)}} = J_1^m, \quad m = 1, 2, \ldots, 7,$$
$$\int_{|\xi|}^{\delta} \frac{t\arcsin\left(\frac{t}{\tilde{x}_0}\right)dt}{(\tilde{x}_0^2-t^2)^m\sqrt{(\tilde{x}_0^2-t^2)(t^2-\xi^2)}} = J_2^m, \quad m = 1, 2, \ldots, 7;$$

(A.II.2.c-d)

$$\int_{|\xi|}^{\delta} \frac{dt}{(\tilde{x}_0^2 - t^2)^m \sqrt{t^2 - \xi^2}} = J_3^m, \quad m = 0, 1, 2, \ldots, 7,$$

$$\int_{|\xi|}^{\delta} \frac{t^m dt}{\sqrt{t^2 - \xi^2}} = J_4^m, \quad m = 1, 2, \ldots, 7;$$

(A.II.3.a-p)

$$S_1 = \overset{0}{A}\tilde{r}_0^2 \tilde{x}_0, \quad S_2 = -\frac{3}{2}\tilde{x}_0\left(\overset{1}{P} - \frac{1}{2\bar{\Delta}^{(4)}} P_4^4\right),$$

$$S_3 = \frac{5}{2}\tilde{x}_1\left\{\frac{3}{8}\left(\frac{1}{\bar{\Delta}^{(4)}} P_4^3 - \frac{1}{\bar{\Delta}^{(6)}} P_6^4\right) + \tilde{x}_0^2\left(\overset{1}{P} - \frac{1}{2\bar{\Delta}^{(4)}} P_4^4\right)\right\},$$

$$S_4 = -\frac{35}{8}\tilde{x}_0\left\{\frac{1}{4\bar{\Delta}^{(6)}} P_6^3 + \tilde{x}_0^2\left(\frac{1}{\bar{\Delta}^{(4)}} P_4^3 - \frac{1}{\bar{\Delta}^{(6)}} P_6^4\right)\right\},$$

$$S_5 = \frac{63}{16}\tilde{x}_0^3\left\{\frac{5}{2\bar{\Delta}^{(6)}} P_6^3 + \tilde{x}_0^2\left(\frac{1}{\bar{\Delta}^{(4)}} P_4^3 - \frac{1}{\bar{\Delta}^{(6)}} P_6^4\right)\right\},$$

$$S_6 = -\frac{4815}{224}\frac{\tilde{x}_0^5}{\bar{\Delta}^{(6)}} P_6^3, \quad S_7 = \frac{397}{32}\frac{\tilde{x}_0^7}{\bar{\Delta}^{(6)}} P_6^3,$$

$$S_8 = \frac{1}{14}\frac{\tilde{x}_0^{-7}}{\bar{\Delta}^{(6)}} P_6^3 + \frac{1}{10}\tilde{x}_0^{-5}\left(\frac{1}{\bar{\Delta}^{(4)}} P_4^3 - \frac{1}{\bar{\Delta}^{(6)}} P_6^4\right)$$
$$+ \frac{1}{3}\tilde{x}_0^{-3}\left(\overset{1}{P} - \frac{1}{2\bar{\Delta}^{(4)}} P_4^4\right) + \tilde{x}_0^{-1}\overset{0}{A}\tilde{r}_1^2;$$

$$S_9 = -\frac{1}{6}\left\{\frac{1}{70}\frac{\tilde{x}_0^{-5}}{\bar{\Delta}^{(6)}} P_6^3 + \frac{1}{20}\tilde{x}_0^{-3}\left(\frac{1}{\bar{\Delta}^{(4)}} P_4^3 - \frac{1}{\bar{\Delta}^{(6)}} P_6^4\right)\right.$$
$$\left. + \tilde{x}_0^{-1}\left(\overset{1}{P} - \frac{1}{2\bar{\Delta}^{(4)}} P_4^4\right) + 6\tilde{x}_0\overset{0}{A}\tilde{r}_1^2\right\},$$

$$S_{10} = \frac{1}{3}\left\{-\frac{1}{560}\frac{\tilde{x}_0^{-3}}{\bar{\Delta}^{(6)}} P_6^3 + \frac{7}{80}\tilde{x}_0^{-1}\left(\frac{1}{\bar{\Delta}^{(4)}} P_4^3 - \frac{1}{\bar{\Delta}^{(4)}} P_6^4\right) + 7\tilde{x}_0\left(\overset{1}{P} - \frac{1}{2\bar{\Delta}^{(4)}} P_4^4\right)\right.,$$

$$S_{11} = -\frac{1}{2}\left\{\frac{71}{1680}\frac{\tilde{x}_0^{-1}}{\bar{\Delta}^{(6)}} P_6^3 + \frac{449}{120}\tilde{x}_0\left(\frac{1}{\bar{\Delta}^{(4)}} P_4^3 - \frac{1}{\bar{\Delta}^{(6)}} P_6^4\right)\right.$$
$$\left. + 5\tilde{x}_0^3\left(\overset{1}{P} - \frac{1}{2\bar{\Delta}^{(4)}} P_4^4\right)\right\},$$

$$S_{12} = \frac{1}{16}\tilde{x}_0\left\{\frac{281}{70\bar{\Delta}^{(6)}} P_6^3 - 91\tilde{x}_0^2\left(\frac{1}{\bar{\Delta}^{(4)}} P_4^3 - \frac{1}{\bar{\Delta}^{(6)}} P_6^4\right)\right\},$$

$$S_{13} = \frac{1}{8}\tilde{x}_0^3\left\{-\frac{611}{5\bar{\Delta}^{(6)}} P_6^3 + \frac{355}{6}\tilde{x}_0^2\left(\frac{1}{\bar{\Delta}^{(4)}} P_4^3 - \frac{1}{\bar{\Delta}^{(6)}} P_6^4\right)\right\},$$

$$S_{14} = \frac{209}{8}\frac{\tilde{x}_0^5}{\bar{\Delta}^{(6)}}P_6^3, \quad S_{15} = -\frac{429}{32}\frac{\tilde{x}_0^7}{\bar{\Delta}^{(6)}}P_6^3,$$

$$S_{16} = \frac{\pi}{2}\left\{\overset{0}{P} + \tilde{x}_0^2\left(\overset{2}{P} + \frac{1}{2\bar{\Delta}^{(4)}}P_4^5\right) + \frac{1}{2}\tilde{x}_0^4\left(\frac{1}{\bar{\Delta}^{(6)}}P_6^5 - \frac{1}{\bar{\Delta}^{(4)}}P_4^6\right) - \frac{1}{2}\frac{\tilde{x}_0^6}{\bar{\Delta}^{(6)}}P_6^6\right\};$$

$$S_{17} = \tilde{x}_0\left\{2\left(\overset{2}{P} + \frac{1}{2\bar{\Delta}^{(4)}}P_4^5\right) + 2\tilde{x}_0^2\left(\frac{1}{\bar{\Delta}^{(6)}}P_6^5 - \frac{1}{\bar{\Delta}^{(4)}}P_4^6\right) - 3\frac{\tilde{x}_0^4}{\bar{\Delta}^{(6)}}P_6^6\right\},$$

$$S_{18} = \frac{\pi}{2}\left\{\overset{2}{P} + \frac{1}{2\bar{\Delta}^{(4)}}P_4^5 + \frac{3}{2}\tilde{x}_0^2\left(\frac{1}{\bar{\Delta}^{(6)}}P_6^5 - \frac{1}{\bar{\Delta}^{(4)}}P_4^6\right) - \frac{15}{4}\frac{\tilde{x}_0^4}{\bar{\Delta}^{(6)}}P_6^6\right\},$$

(A.II.3.q-v)
$$S_{19} = \frac{4}{3}\tilde{x}_0\left\{\frac{1}{\bar{\Delta}^{(6)}}P_6^5 - \frac{1}{\bar{\Delta}^{(4)}}P_4^6 - 5\frac{\tilde{x}_0^2}{\bar{\Delta}^{(6)}}P_6^6\right\},$$

$$S_{20} = \frac{3\pi}{32}\left\{\frac{1}{\bar{\Delta}^{(6)}}P_6^5 - \frac{1}{\bar{\Delta}^{(4)}}P_4^6 - 15\frac{\tilde{x}_0^2}{\bar{\Delta}^{(6)}}P_6^6\right\},$$

$$S_{21} = -\frac{8}{5}\frac{\tilde{x}_0}{\bar{\Delta}^{(6)}}P_6^6, \quad S_{22} = -\frac{15}{64}\frac{\pi}{\bar{\Delta}^{(6)}}P_6^6;$$

$$T_1 = 0, \quad T_2 = -\frac{3}{2}\tilde{x}_0\left(\overset{2}{Q} - \frac{1}{2\bar{\Delta}^{(3)}}P_3^4\right), \quad T_3 = \frac{15}{16}\tilde{x}_0\left(\frac{1}{\bar{\Delta}^{(3)}}P_3^3 - \frac{1}{\bar{\Delta}^{(5)}}P_5^4\right),$$

$$T_4 = -\frac{35}{32}\tilde{x}_0\left\{\frac{1}{\bar{\Delta}^{(5)}}P_5^3 + 2\tilde{x}_0^2\left(\frac{1}{\bar{\Delta}^{(3)}}P_3^3 - \frac{1}{\bar{\Delta}^{(5)}}P_5^4\right)\right\},$$

$$T_5 = \frac{105}{16}\frac{\tilde{x}_0^3}{\bar{\Delta}^{(5)}}P_5^3, \quad T_6 = -\frac{231}{32}\frac{\tilde{x}_0^5}{\bar{\Delta}^{(5)}}P_5^3, \quad T_7 = 0,$$

$$T_8 = \frac{\tilde{x}_0}{2}\left\{2\left(\overset{1}{Q} + \frac{1}{2\bar{\Delta}^{(3)}}P_3^5\right) + \tilde{x}_0^2\left(\frac{1}{\bar{\Delta}^{(5)}}P_5^5 - \frac{1}{\bar{\Delta}^{(3)}}P_3^6\right) - \frac{\tilde{x}_0^4}{\bar{\Delta}^{(5)}}P_5^6\right\},$$

$$T_9 = -\frac{\tilde{x}_0^{-1}}{2}\left\{\frac{1}{30}\frac{\tilde{x}_0^{-4}}{\bar{\Delta}^{(5)}}P_5^3 + \frac{\tilde{x}_0^{-2}}{12}\left(\frac{1}{\bar{\Delta}^{(3)}}P_3^3 - \frac{1}{\bar{\Delta}^{(5)}}P_5^4\right) + \left(\overset{2}{Q} - \frac{1}{2\bar{\Delta}^{(3)}}P_3^4\right)\right\},$$

(A.II.4.a-p)
$$T_{10} = \frac{1}{2}\left\{-\frac{\tilde{x}_0^{-3}}{40\bar{\Delta}^{(5)}}P_5^3 + \frac{\tilde{x}_0^{-1}}{24}\left(\frac{1}{\bar{\Delta}^{(3)}}P_3^3 - \frac{1}{\bar{\Delta}^{(5)}}P_5^4\right) + 3\tilde{x}_0\left(\overset{2}{Q} - \frac{1}{2\bar{\Delta}^{(3)}}P_3^4\right)\right\},$$

$$T_{11} = \frac{1}{3}\left\{-\frac{19}{160}\frac{\tilde{x}_0^{-1}}{\bar{\Delta}^{(5)}}P_5^3 + 5\tilde{x}_0\left(\frac{1}{\bar{\Delta}^{(3)}}P_3^3 - \frac{1}{\bar{\Delta}^{(5)}}P_5^4\right)\right\},$$

$$T_{12} = \frac{\tilde{x}_0}{16}\left\{\frac{371}{10\bar{\Delta}^{(5)}}P_5^3 - \frac{55}{3}\tilde{x}_0^2\left(\frac{1}{\bar{\Delta}^{(3)}}P_3^3 - \frac{1}{\bar{\Delta}^{(5)}}P_5^4\right)\right\}, \quad T_{13} = -\frac{287}{32}\frac{\tilde{x}_0^3}{\bar{\Delta}^{(5)}}P_5^3;$$

$$T_{14} = \frac{231}{32}\frac{\tilde{x}_0^5}{\bar{\Delta}^{(5)}}P_5^3, \quad T_{15} = 0,$$

$$T_{16} = \frac{\pi}{8}\left\{2\left(\overset{1}{Q} + \frac{1}{2\bar{\Delta}^{(3)}}P_3^5\right) + 3\tilde{x}_0^2\left(\frac{1}{\bar{\Delta}^{(5)}}P_5^5 - \frac{1}{\bar{\Delta}^{(3)}}P_3^6\right) - 5\frac{\tilde{x}_0^4}{\bar{\Delta}^{(5)}}P_5^6\right\},$$

(A.II.4.q-v)
$$T_{17} = \tilde{x}_0 \left\{ \frac{1}{\bar{\Delta}^{(5)}} P_5^5 - \frac{1}{\bar{\Delta}^{(3)}} P_3^6 - \frac{10}{3} \frac{\tilde{x}_0^2}{\bar{\Delta}^{(5)}} P_5^6 \right\},$$

$$T_{18} = \frac{3\pi}{16} \left\{ \frac{1}{2} \left(\frac{1}{\bar{\Delta}^{(5)}} P_5^5 - \frac{1}{\bar{\Delta}^{(3)}} P_3^6 \right) - 5 \frac{\tilde{x}_0^2}{\bar{\Delta}^{(5)}} P_5^6 \right\},$$

$$T_{19} = -\frac{4}{3} \frac{\tilde{x}_0}{\bar{\Delta}^{(5)}} P_5^6, \quad T_{20} = -\frac{5\pi}{64\bar{\Delta}^{(5)}} P_5^6, \quad T_{21} = 0, \quad T_{22} = 0.$$

References

1. P. C. HUANG, VAN DER MAAS, WADCTR 59-2, 1959.
2. Z. OLESIAK, I. N. SNEDDON, Arch. Rat. Mech. Anal., **4**, 238, 1960.
3. G. C. SIH, J. Appl. Mech., **29**, 587, 1962.
4. A. L. FLORENCE, J. N. GOODIER, Int. J. Eng. Sci., **1**, 533, 1963.
5. J. N. GOODIER, A. L. FLORENCE, Proc. 11th Int. Congr. Appl. Mech., Munich 1964.
6. A. F. EMERY, J. Basic Eng., **87**, 45, 1965.
7. M. HIEKE, F. LOGES, Z. Angew. Phys., **22**, 14, 1966.
8. M. K. KASSIR, G. C. SIH, *Development in Theoretical and Applied Mechanics*, **3**, edited by W. SHAW, 117, 1967.
9. E. J. BROWN, F. ERDOGAN, Int. J. Eng. Sci., **6**, 517, 1968.
10. M. K. KASSIR, Int. J. Eng. Sci., **7**, 769, 1969.
11. M. SVOBODA, Int. J. Fracture Mech., **5**, 315, 1969.
12. J. G. BLAUEL, Ph. D. Dissertation, University of Karlsruhe, 1970.
13. E. BRUY, Ph. D. Dissertation, University of Stuttgart, 1973.
14. A. M. BREGMAN, M. K. KASSIR, Int. J. Fracture, **10**, 87, 1974.
15. K. HERRMANN, GAMM-Conference Bochum 1974, Mech. Res. Comm., **1**, 355, 1974.
16. A. H. LACHENBRUCH, J. Geophys. Res., **66**, 4273, 1961.
17. F. KERKHOF, Naturwissenschaften, **40**, 478, 1953.
18. F. KERKHOF, H. DREIZLER, Glastechn. Ber., **29**, 459, 1956.
19. E. KRÖNER, Ergebnisse der angew. Mathematik, Heft 5, 32, Springer-Verlag, Berlin 1958.
20. K. HERRMANN, M. HIEKE, Witold NOWACKI Anniversary Volume, 61, Wolters-Noordhoff Publishing, 1971.
21. A. H. ENGLAND, A. E. GREEN, Proc. Camb. Phil. Soc., **59**, 489, 1963.
22. J. R. RICE, J. Appl. Mech., **35**, 379, 1968.
23. R. K. LEVERENZ, Int. J. of Fracture Mech., **8**, 311, 1972.
24. I. M. RYSHIK, I. S. GRADSTEIN, *Integral Tables*, Deutscher Verlag der Wissenschaften, Berlin 1957.
25. W. GRÖBNER, N. HOFREITER, *Integral Table*, Part I, Springer-Verlag, Wien 1961.
26. I. N. BRONSTEIN, K. A. SEMENDJAJEW, *Taschenbuch der Mathematik*, Verlag H. Deutsch, Zürich und Frankfurt/M. 1968.

UNIVERSITÄT KARLSRUHE (TH)
INSTITUT FÜR TECHNISCHE MECHANIK UND FESTIGKEITSLEHRE.

Received Mai 25, 1975.